Silicon beam splitter for far-infrared and terahertz spectroscopy

Christopher C. Homes,[1,2,*] G. Lawrence Carr,[3] Ricardo P. S. M. Lobo,[2] Joseph D. LaVeigne,[4,5] and David B. Tanner[4]

[1]Condensed Matter Physics and Materials Science Department, Brookhaven National Laboratory, Upton, New York 11973, USA

[2]Laboratoire Photons et Matière, École Supérieure de Physique et Chimie Industrielles, Centre National de la Recherche Scientifique, Unité Propre de Recherche 5, Universite Pierre et Marie Curie, 10 rue Vauquelin, 75231 Paris Cedex 5, France

[3]National Synchrotron Light Source, Brookhaven National Laboratory, Upton, New York 11973, USA

[4]Department of Physics, University of Florida, Gainesville, Florida 32611, USA

[5]Currently with Santa Barbara Infrared, Incorporated, 30 South Calle Cesar Chavez, Suite D, Santa Barbara, California 93103, USA

*Corresponding author: homes@bnl.gov

Silicon beam splitters several millimeters thick offer numerous advantages over thin freestanding dielectric beam splitters. For routine spectroscopy for which resolutions of better than $1 \, \text{cm}^{-1}$ are not required, a silicon beam splitter can replace several Mylar beam splitters to span the entire far-infrared region. In addition to superior long-wavelength performance that extends well into the terahertz region, the silicon beam splitter has the additional advantage that its efficiency displays little polarization dependence. © 2007 Optical Society of America

OCIS codes: 120.3180, 300.6340.

1. Introduction

Spectroscopic measurements in the infrared optical region (energies below approximately 0.1 eV or wavelengths greater than approximately 10 μm) are complicated by the lack of suitable materials for optical windows and beam splitters. The choice of beam splitters is particularly challenging; it is the key component in Fourier-transform infrared (FTIR) spectroscopy [1–3]. The beam splitter efficiency determines the frequency coverage and accuracy of these spectrometers. In general, beam splitters used in Michelson-type spectrometers are either polarizing wire grids, freestanding dielectric films, or thin or thick substrate-coated beam splitters. The polarizing grid responds to just one polarization and is limited to wavelengths longer than the grid separation, effec-tively restricting it to the far-infrared region. The alkali–halide materials that are typically used to support dielectric coatings in mid-infrared beam splitters are opaque below ≃30 meV. Other materials, such as thin films of polypropylene or polyethylene, are transparent over much of the far-infrared region and make excellent optical windows [4,5]; however, the low refractive index ($n \simeq 1.2$) limits their usefulness as beam splitters. In modern Michelson rapid-scan FTIR spectrometers, thin polyethylene terephthalate [(PET) also known commercially as Mylar] dielectric beam splitters are a common choice. However, one of the problems associated with PET beam splitters is the overall low efficiency. These beam splitters function by means of the interference of multiple internally reflected beams; therefore the reflectance (and efficiency) is zero when the interference condition is destructive for the reflected beams. In the far-infrared region, a combination of beam splitters of differing thicknesses must be employed to

yield a series of discrete frequency regions, which are then merged to form a continuous spectrum. It has been recognized recently that thick silicon beam splitters offer numerous advantages over PET beam splitters for routine spectroscopy; however, they are not widely available. We discuss the advantages of thick Si over PET beam splitters and examine the results in a Genzel-type [6] FTIR spectrometer.

2. Beam Splitter Response

The relative efficiency of a beam splitter at a given frequency is given by $\varepsilon = 4R_0T_0$, where R_0 and T_0 are the reflectance and transmittance of the beam splitter, respectively [7]. For this discussion it is convenient to describe the frequency ω in wavenumbers in units of reciprocal centimeters; wavenumbers scale linearly with photon energy (1 eV $\simeq 8066$ cm^{-1}) and are just the inverse of the vacuum wavelength, measured in centimeters. The maximum efficiency is found when $R_0 = T_0 = 0.5$, which yields $\varepsilon = 1$. For a freestanding, nonabsorbing, parallel-sided, thin dielectric material, the frequency dependence of the reflectance and transmittance are

$$R_0 = \frac{2R^2(1 - \cos \delta)}{1 + R^2 - 2R \cos \delta}, \quad (1)$$

$$T_0 = \frac{(1 - R^2)}{1 + R^2 - 2R \cos \delta}, \quad (2)$$

where $\delta = 4\pi\omega nd \cos \theta_t$ is the relative phase shift between two adjacent emerging rays, d is the thickness of the film, n is its refractive index, θ_t is the angle of the beam inside the film to the surface normal, and R is the single-bounce reflectance of the material (for a nonzero angle of incidence both R_0 and T_0 depend on the polarization, as discussed below).

These functions oscillate with period δ; the reflectance is maximum when the transmittance is minimum and vice versa. Together these functions satisfy the condition $R_0 + T_0 = 1$. Thus, the beam splitter efficiency has minima at $\delta = 2m\pi$ for $m = 1, 2, 3, \ldots$ and maxima near $\delta = (2m - 1)\pi$; we usually restrict our use of the beam splitter to the first interval. Note that, if $R_0 > 0.5$ at the frequencies where $\delta = (2m - 1)\pi$, there will be a local minimum at that value of δ, with maxima on either side.

Radiation polarized with its electric field parallel to the plane of incidence is denoted by p; radiation polarized with its electric field perpendicular to the plane of incidence is denoted by s. For any nonzero angle of incidence at the beam splitter, the reflectance for p- and s-polarized radiation has different forms

$$R_p = \frac{\tan^2(\theta_i - \theta_t)}{\tan^2(\theta_i + \theta_t)}, \quad (3)$$

$$R_s = \frac{\sin^2(\theta_i - \theta_t)}{\sin^2(\theta_i + \theta_t)}, \quad (4)$$

Table 1. Efficiencies for a PET Beam Splitter (n = 1.6) and for a Si Beam Splitter (n = 3.4)[a]

Material	Polarization	$\theta_i = 45°$			$\theta_i = 30°$		
		R_0	T_0	$4R_0T_0$	R_0	T_0	$4R_0T_0$
PET	p	0.052	0.95	0.20	0.13	0.87	0.45
	s	0.37	0.63	0.93	0.26	0.74	0.77
	None	0.21	0.79	0.56	0.20	0.80	0.61
Si	p	0.51	0.49	1.00	0.63	0.37	0.93
	s	0.83	0.17	0.56	0.77	0.23	0.71
	None	0.67	0.33	0.78	0.70	0.30	0.82

[a]At the wavelength for which reflectance is a maximum and transmittance is a minimum. The quantities are calculated for p and s polarizations at angles of incidence of 30° and 45°.

where θ_i and θ_t are the angles of incidence and transmission, respectively, and are related by $n = \sin \theta_i / \sin \theta_t$. The refractive index of PET is $n \simeq 1.6$, and the index of absorption $k \approx 0$ over most of the far-infrared region.

The relative maximum beam splitter efficiencies of a PET beam splitter for the s and p polarizations are calculated for $\theta_i = 45°$ (as occurs in a classic Michelson interferometer), as well as the lower angle $\theta_i = 30°$ now found in many modern interferometers; these results are summarized in Table 1. Table 1 shows the quantities at the wavelength at which reflectance is a maximum and transmittance is a minimum. Because of the large difference in efficiencies for the two polarizations, a Michelson interferometer equipped with a PET beam splitter is far more effective for s-polarized than for p-polarized radiation. The strong polarization dependence of the PET beam splitters, especially near 45°, limits their use when polarization studies are necessary. As indicated in Table 1, the difference between the s and the p polarizations for PET beam splitters could be reduced
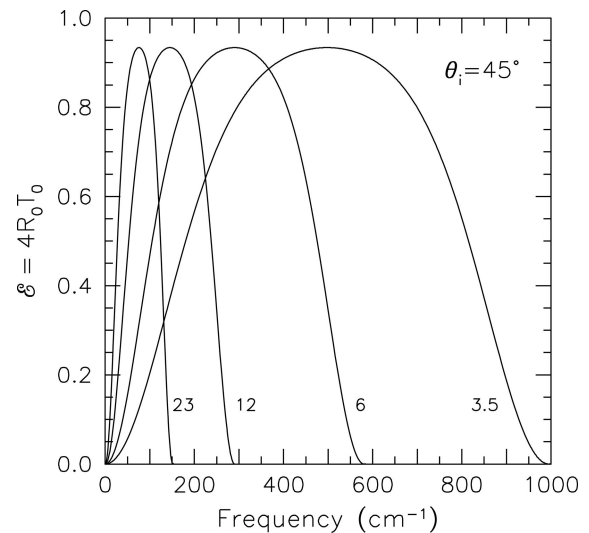

Fig. 1. Beam splitter efficiency versus frequency in a standard Michelson spectrometer ($\theta_i = 45°$) of 3.5, 6, 12, and 23 μm PET beam splitters as a function of frequency for s-polarized radiation.

by decreasing θ_i, with a slight increase in the overall efficiency [8].

Figure 1 shows the variation in the calculated efficiency of four common PET beam splitters as a function of frequency for s-polarized radiation in a conventional Michelson interferometer. Only the first cycle of the interference pattern is shown for each. To cover the entire far-infrared region from 10 to 700 cm^{-1} using PET beam splitters with a beam splitter efficiency greater than 0.5 requires at a minimum all four beam splitters. At low energies (<50 cm^{-1}), where the efficiency of these beam splitters is poor and blackbody sources are weak, measurements become difficult.

3. Silicon Beam Splitter

The beam splitter efficiency can be improved if a material with a larger refractive index than PET, such as silicon ($n \simeq 3.4$) [9] or germanium ($n \simeq 4$), [10] is employed. Figure 2 shows the calculated variation of R_0 for both s- and p-polarized radiation (R_{0s} and R_{0p}, respectively) as a function of the refractive index of the material from which the beam splitter is fabricated, as well as several different angles of incidence, $\theta_i = 45°$, 30°, and 15°. The difference between the values of R_{0s} and R_{0p} can be decreased considerably by reducing the angle of incidence at the beam splitter. Table 1 lists calculated reflectance, transmittance, and beam splitter efficiencies for silicon, again at the wavelength at which reflectance is a maximum. Because the reflectance exceeds 0.5 at this wavelength, there are wavelengths for which the efficiency is 1.0 nearby.

If the Si plate is several millimeters thick, the beam splitter response consists of many closely spaced cycles, making the single-channel spectrum
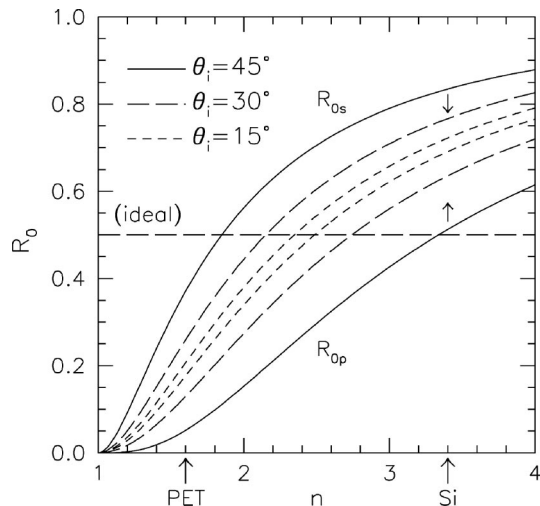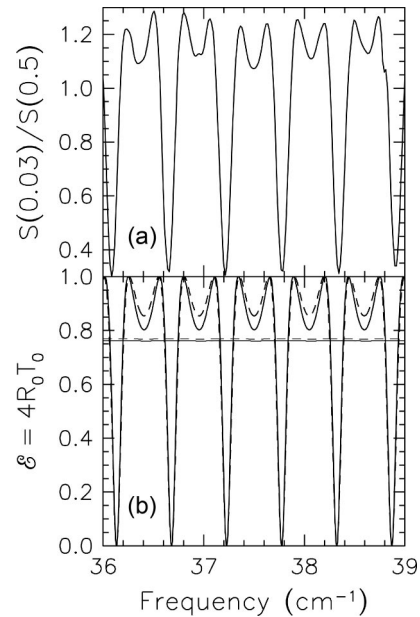

Fig. 3. Experimentally observed ratio of two unpolarized single-channel spectra using a silicon beam splitter in a Genzel-type interferometer ($\theta_i \simeq 15°$) with resolutions of 0.03 and 1 cm^{-1}, shown over a narrow frequency interval in the far infrared. (b) The calculated beam splitter efficiency for a thick piece of silicon ($d \simeq 2.7$ mm, $n \simeq 3.4$) for s- and p-polarized radiation (solid and dashed curves, respectively). The almost structureless horizontal lines drawn with a lighter weight are the result of smoothing the data by use of a Gaussian convolution with a width of 1 cm^{-1}; the solid and dashed curves again denote the s and p polarizations, respectively.

Fig. 2. Variation of R_0 for s- and p-polarized radiation as a function of the refractive index for 45° (solid curve), 30° (long dashed curve), and 15° (short dashed curve) angles of incidence. The values of the refractive index for both PET and Si are indicated. Note that, for a high-index material such as Si, not only are the values for R_0 closer to the ideal value, but the difference between R_{0s} and R_{0p} is much smaller at a reduced angle of incidence (15°) than in a conventional Michelson spectrometer (45°).

$[S(\omega)]$ unsuitable for high resolution spectroscopic applications. To illustrate this point, a thick silicon beam splitter ($d \simeq 2.7$ mm) was examined in a Bruker IFS 113v interferometer. This instrument has two unique aspects: the first is that the light is focused at the beam splitter (unlike a standard Michelson-type interferometer in which the light is collimated), an arrangement that allows for smaller beam splitters; the second is the low angle of incidence at the beam splitter $\theta_i = 15°$, which is close to the optimal angle for PET beam splitters [8] (this instrument is referred to as a Genzel-type spectrometer) [6]. Figure 3(a) shows the ratio of two unpolarized single-channel spectra for the silicon beam splitter measured with experimental resolutions of $\delta\omega = 0.03$ and 1 cm^{-1}; the low resolution spectrum should describe the instrument background, so that the ratio $S(\delta\omega = 0.03$ cm$^{-1})/S(\delta\omega = 1$ cm$^{-1})$ should be a good approximation of the beam splitter efficiency. The beam splitter response has been modeled in Fig. 3(b) for a piece of silicon approximately 2.7 mm thick, a refractive index of $n = 3.4$, and $\theta_i = 15°$ for both s and p polarizations. The spacing of the cycles of $\simeq 0.7$ cm^{-1} observed in the upper panel is reproduced quite well by the calculation, which shows little polarization dependence.

As noted above, this beam splitter is unsuitable when high resolution is required. However, if the

resolution required is less than this spacing between the cycles, then only the average beam splitter response is observed. The horizontal lines in Fig. 3(b) show the beam splitter response after it has been smoothed by applying a Gaussian convolution of $1~\mathrm{cm}^{-1}$ width; the fine structure is removed yielding an essentially flat response with a beam splitter efficiency of $4R_0T_0 \simeq 0.76$ for s-polarized radiation. If this smoothed result is used as a background, the maxima of $\simeq 1.3$ observed in the upper panel is reproduced; the maximum available resolution limits our ability to observe the predicted zeros in the beam splitter response. For resolutions $\delta\omega \gtrsim 1~\mathrm{cm}^{-1}$, this beam splitter therefore has an excellent broadband response, extending to the lowest frequencies. Unlike PET beam splitters for which the p-polarized response is considerably poorer than the s-polarized case, the thick Si beam splitter actually delivers a slightly better performance.

The relative performance of Si and PET beam splitters is accomplished by the comparison of single-channel spectra for which the only experimental parameter that is altered is the type of beam splitter. Figures 4(a) and 4(b) compare the Si beam splitter with 3.5 and 50 μm PET beam splitters, respectively. For these experiments we used a 4.2 K bolometer detector. Long-wavelength pass cold filters restrict the response of the detector to frequencies below approximately 800 and 100 cm^{-1} in the upper and lower panels, respectively. When compared with the thin 3.5 μm PET beam splitter, the Si beam splitter has a somewhat poorer performance $\gtrsim 450~\mathrm{cm}^{-1}$; however, it is dramatically better below approximately 200 cm^{-1}. When compared with a thick 50 μm PET beam splitter, the Si beam splitter has two important advantages; the first is that the Si beam splitter is more efficient at low frequencies, and the second is that it does not suffer the cyclic behavior of the thick PET beam splitter. Thus, the Si beam splitter performs well over the entire far-infrared and terahertz regions (1 THz $\simeq 33.3~\mathrm{cm}^{-1}$) and for routine spectroscopy can effectively replace most PET beam splitters without any corresponding loss of efficiency. Note that the spectra taken at high resolution ($1~\mathrm{cm}^{-1}$) in Fig. 4(b) shows some fine structure at low frequency in both the PET and the Si beam splitters. This effect is due to the composite nature of the bolometer detector; the impedance of the antenna used to collect radiation is not perfectly matched to the impedance of free space, resulting in weak interference fringes [11]. When used with a 1.4 K bolometer detector, the instrument delivers excellent spectral information down to $\approx 5~\mathrm{cm}^{-1}$. (In this case the low-frequency response appears to be detector limited.) In principle, if the sides are highly parallel, the Si beam splitter should operate continuously into the mid-infrared, with the exception of a strong phonon band at $\approx 620~\mathrm{cm}^{-1}$; thick Ge plates are unsuitable for beam splitters because of strong phonon absorption.

Although a thick Si beam splitter is useful for routine spectroscopy, it is unsuitable for high-resolution applications as illustrated in Fig. 3. In principle, many of the advantages of the thick Si beam splitter could be realized in a thin, freestanding version several micrometers thick; this would eliminate the closely spaced cycles and yield a beam splitter response more typical of a thin PET beam splitter. Indeed, this approach has been employed in a solid silicon-wafer beam splitter [12]; however, in this implementation the wafer is wedged and lacks an antireflection coating, resulting in an approximately 30% reduction in efficiency. More recently, it was proposed [13,14] and demonstrated [14,15] that thin layers of silicon can be deposited onto a PET substrate, yielding a high beam splitter efficiency over much of the far-infrared region. In a similar fashion, a thin layer of germanium has been deposited onto a PET substrate, resulting in a multilayer dielectric beam splitter; this beam splitter is commercially available from Bruker Optics [16]. These multilayer beam splitters provide excellent coverage over much of the far infrared with improved performance at long wavelengths, which can be used for high-resolution work. However, even though the Ge/PET beam splitter is far superior to a 6 μm PET beam splitter in the terahertz region (i.e., below 30 cm^{-1}), its efficiency is still poorer than a 50 μm PET beam splitter and is much poorer than the thick Si beam splitter reported here.
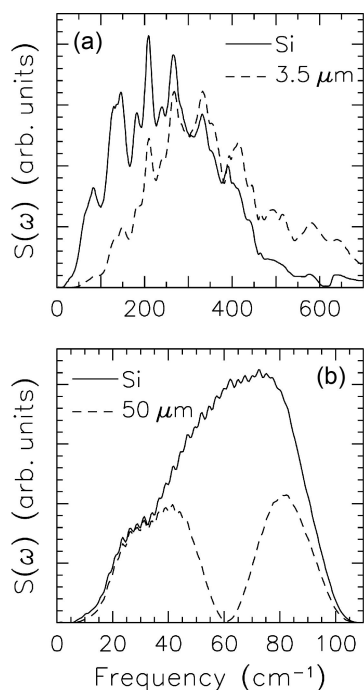

Fig. 4. (a) Comparison of the single-channel spectra for a Si (solid curve) and 3.5 μm PET (dashed curve) beam splitter in a Genzel interferometer spanning much of the far-infrared region (GLOBAR source, liquid helium bolometer detector). The experimental resolution is 2 cm^{-1}. (b) Comparison of the single-channel spectra for a Si (solid curve) and 50 μm PET (dashed curve) beam splitter (Hg arc lamp source, liquid helium bolometer detector with a 100 cm^{-1} low-pass cold filter). The experimental resolution is 1 cm^{-1}. The weak interference fringes observed at low frequency are due to an intrinsic detector effect.

4. Conclusion

A piece of Si several millimeters thick is an excellent beam splitter for use over much of the mid- and far-infrared regions. For routine spectroscopy for which resolutions of no greater than $\simeq 1\ \mathrm{cm}^{-1}$ are required, a Si beam splitter can effectively replace most PET beam splitters. The Si beam splitter operates effectively well into the terahertz region (0.2–10 THz). A final advantage is that the Si beam splitter displays an almost total lack of polarization dependence at modest incidence angles.

References

1. J. L. Deuzé and A. L. Fymat, "Instrumentation optimization in Fourier spectroscopy. 1: Far infrared beam splitters," Appl. Opt. **13,** 1807–1813 (1974).
2. D. R. Smith and E. V. Loewenstein, "Far-infrared thin-film beam splitters: calculated properties," Appl. Opt. **14,** 2473–2475 (1975).
3. G. Kampffmeyer and A. Pfeil, "Self-supporting thin-film beam splitter for far-infared interferometers," Appl. Phys. A **14,** 313–317 (1977).
4. D. R. Smith and E. V. Loewenstein, "Optical constants of far infrared materials. 3: Plastics," Appl. Opt. **14,** 1335–1341 (1975).
5. D. Labrie, I. Booth, M. L. W. Thewalt, and B. P. Clayman, "Use of polypropylene film for infrared cryostat windows," Appl. Opt. **25,** 171–172 (1986).
6. L. Genzel and J. Kuhl, "Tilt-compensated Michelson interferometer for Fourier transform spectroscopy," Appl. Opt. **17,** 3304–3008 (1978).
7. R. J. Bell, *Introductory Fourier Transform Spectroscopy* (Academic, 1972).
8. D. A. Naylor, R. T. Boreiko, and T. A. Clark, "Mylar beam splitter efficiency in far infrared interferometers: angle of incidence and absorption effects," Appl. Opt. **17,** 1055–1058 (1978).
9. D. F. Edwards, "Silicon (Si)," in *Handbook of Optical Constants of Solids,* E. D. Palik, ed. (Academic, 1985), pp. 547–569.
10. R. F. Potter, "Germanium (Ge)," in *Handbook of Optical Constants of Solids,* E. D. Palik, ed. (Academic, 1985), pp. 465–478.
11. K. E. Kornelsen, M. Dressel, J. E. Eldridge, M. J. Brett, and K. L. Westra, "Far-infrared optical absorption and reflectivity of a superconducting NbN film," Phys. Rev. B **44,** 11882–11887 (1991).
12. D. W. Vidrine and C. R. Anderson, "Silicon beamsplitter," U.S. patent 4,632,553 (30 December 1986).
13. J. A. Dobrowolski and W. A. Traub, "New designs for far-infrared beam splitters," Appl. Opt. **35,** 2934–2946 (1996).
14. N. L. Rowell and E. A. Wang, "Bilayer free-standing beam splitter for Fourier transform infrared spectrometry," Appl. Opt. **35,** 2927–2933 (1996).
15. N. L. Rowell and E. A. Wang, "Silicon coated mylar beamsplitter," U.S. patent 5,558,934 (24 September 1996).
16. Bruker Optik GmbH, Rudolf-Plank-Strasse 27, Ettlingen, Germany.